



**HAL**  
open science

## Gravity wave spectra parameters in 2003 retrieved from stellar scintillation measurements by GOMOS

Viktorija F. Sofieva, A.S. Gurvich, Francis Dalaudier

► **To cite this version:**

Viktorija F. Sofieva, A.S. Gurvich, Francis Dalaudier. Gravity wave spectra parameters in 2003 retrieved from stellar scintillation measurements by GOMOS. *Geophysical Research Letters*, 2009, 36 (5), pp.L05811. 10.1029/2008GL036726 . hal-00367488

**HAL Id: hal-00367488**

**<https://hal.science/hal-00367488>**

Submitted on 1 Feb 2016

**HAL** is a multi-disciplinary open access archive for the deposit and dissemination of scientific research documents, whether they are published or not. The documents may come from teaching and research institutions in France or abroad, or from public or private research centers.

L'archive ouverte pluridisciplinaire **HAL**, est destinée au dépôt et à la diffusion de documents scientifiques de niveau recherche, publiés ou non, émanant des établissements d'enseignement et de recherche français ou étrangers, des laboratoires publics ou privés.

# Gravity wave spectra parameters in 2003 retrieved from stellar scintillation measurements by GOMOS

V. F. Sofieva,<sup>1</sup> A. S. Gurvich,<sup>2</sup> and F. Dalaudier<sup>3</sup>

Received 19 November 2008; revised 17 January 2009; accepted 2 February 2009; published 11 March 2009.

[1] Using satellite measurements of stellar scintillation allows quantifying gravity waves (GW) in the stratosphere and their breaking into turbulence. GW and turbulence spectra parameters are retrieved by fitting modeled scintillation spectra to measured spectra. We use a two-component spectral model of air density irregularities: the first component corresponds to the gravity wave spectrum, while the second one describes patches of locally isotropic turbulence. In this paper, we show global distributions and seasonal variations of the GW spectra parameters (structure characteristic, inner and outer scales) retrieved from GOMOS/Envisat scintillation measurements in 2003, for altitudes 30–50 km, and discuss peculiarities of these distributions. The use of outer scale estimations has enabled us to obtain self-consistent estimates of GW potential energy  $E_p$  per unit mass. GW parameters retrieved from scintillations are in good agreement with those from other measurements at overlapping altitudes and locations. **Citation:** Sofieva, V. F., A. S. Gurvich, and F. Dalaudier (2009), Gravity wave spectra parameters in 2003 retrieved from stellar scintillation measurements by GOMOS, *Geophys. Res. Lett.*, 36, L05811, doi:10.1029/2008GL036726.

## 1. Introduction

[2] The use of satellite observations of stellar scintillation for studying small-scale irregularities of the Earth atmosphere is a relatively new approach that allows quantification of the activity of small-vertical-scale gravity waves and their breaking into turbulence [Gurvich and Kan, 2003a, 2003b]. After the launch of the GOMOS (Global Ozone Monitoring by Occultation of Stars) instrument on board the Envisat satellite in March 2002, scintillation measurements became available with global coverage.

[3] A method for reconstruction of GW and turbulence spectra parameters from stellar scintillations has been recently developed and adapted to GOMOS measurements [Sofieva *et al.*, 2007a]. For this analysis, data of the GOMOS red ( $\sim 672$  nm) photometer, which records stellar scintillations continuously at 1 kHz sampling frequency in a limb-viewing geometry, are used. The description of the spectral model and the method for the reconstruction of its parameters are presented in Section 2 of our paper.

[4] First applications of this method have already yielded interesting results. For example, there is indication of gravity wave breaking related to the polar night jet [Sofieva

*et al.*, 2007b]. First global distributions of the turbulence structure characteristic  $C_T^2$  at altitudes 30–50 km in all four seasons of year 2003 were obtained [Gurvich *et al.*, 2007].

[5] In this paper, we present a characterization of anisotropic irregularities of air density in the stratosphere, which are assumed to be generated by gravity waves, in two seasons of 2003, as obtained from GOMOS scintillation measurements. This analysis has two main objectives: (i) to demonstrate the capabilities of the novel method for studying stratospheric air density irregularities, and (ii) to present a kind of geophysical validation for the new, scintillation, method by comparing the retrieved GW parameters, their global distributions and their seasonal variations with those obtained from other instruments and methods.

## 2. Reconstruction of GW and Turbulence Spectra Parameters: A Brief Description of the Method

[6] Scintillations are caused by air density irregularities along the line of sight, and they contain therefore information about small-scale processes in the atmosphere [Tatarskii, 1971]. However, the retrieval of this information is a complicated task, because a three-dimensional (3D) distribution of air density irregularities is sought from one-dimensional scintillation measurements. In order to avoid severe ill-posedness, the following approach is used: the 3D spatial spectrum of irregularities is parameterized, and the essential parameters of the spectral model are retrieved by fitting the modeled scintillation spectra to the measured ones. In the retrievals, the modeled scintillation spectra are computed using the theory of wave propagation in a random media with irregularities having the assumed spectral properties.

[7] The velocity of the line of sight within the atmosphere is 3–7 km/s. This is many times greater than velocities of any atmospheric motion and enables one to study spatial structure of irregularities ignoring their evolution during the observation time. We describe the structure of relative fluctuations  $\nu = \frac{N - \langle N \rangle}{\langle N \rangle}$  of refractivity  $N$  (angular brackets denote hereafter the statistical mean) via its 3D spectral density  $\Phi_\nu(\boldsymbol{\kappa})$ ,  $\boldsymbol{\kappa} = \{\kappa_x, \kappa_y, \kappa_z\}$  being a wave vector, where  $z$  is the vertical coordinate. Relative refractivity fluctuations are equal to relative fluctuations of air density and  $\nu = -\frac{T - \langle T \rangle}{\langle T \rangle}$ ,  $T$  being temperature, if small-scale pressure fluctuations are ignored. We represent  $\Phi_\nu$  as a sum of two statistically independent components: anisotropic,  $\Phi_W$ , and isotropic,  $\Phi_K$  [Gurvich and Kan, 2003a; Sofieva *et al.*, 2007a]:

$$\Phi_\nu = \Phi_W + \Phi_K \quad (1)$$

The first component  $\Phi_W$  corresponds to anisotropic irregularities generated by a random ensemble of internal

<sup>1</sup>Finnish Meteorological Institute, Helsinki, Finland.

<sup>2</sup>A. M. Oboukhov Institute of Atmospheric Physics, Moscow, Russia.

<sup>3</sup>LATMOS, Verrières-le-Buisson, France.

gravity waves [e.g., *Smith et al.*, 1987]. For parameterization of this component, a 3D spectrum is used:

$$\Phi_W = C_W \eta^2 (\kappa_z^2 + \eta^2 \kappa_\perp^2 + \kappa_0^2)^{-5/2} \varphi\left(\frac{\kappa}{\kappa_W}\right),$$

$$\kappa^2 = \eta^2 \kappa_\perp^2 + \kappa_z^2, \kappa_\perp^2 = \kappa_x^2 + \kappa_y^2 \quad (2)$$

where  $C_W$  is the structure characteristic defining the intensity of the anisotropic irregularities. The anisotropy coefficient  $\eta$  defines the oblateness of the irregularities. The function  $\varphi(\xi)$  in equation (2) describes the decay of  $\Phi_W$  at  $\kappa > \kappa_W$  [*Gurvich and Kan*, 2003a]. The characteristic wave number  $\kappa_0$  defines the low wave number limit of the  $\kappa^{-5}$  spectrum. In this sense the value of  $L_0 = \frac{2\pi}{\kappa_0}$  can be taken as an estimate of the vertical outer scale of the anisotropic spectrum  $\Phi_W$ , analogously to the outer scale of turbulence. Although the 3D spectral model for GW is more complicated, the model equation (2) takes into account all the important physical parameters controlling the shape of scintillation spectra.

[8] The associated 1D vertical spectrum of relative density (or temperature) fluctuations  $V(\kappa_z) = \int_{-\infty}^{\infty} \int_{-\infty}^{\infty} \Phi_W d\kappa_x d\kappa_y$  for  $\kappa_z < \kappa_W$  is then

$$V(\kappa_z) \approx \frac{2\pi}{3} C_W (\kappa_z^2 + \kappa_0^2)^{-3/2}. \quad (3)$$

Note that the expression for  $V(\kappa_z)$  does not depend on the anisotropy coefficient  $\eta$ . The choice of the function  $\varphi$  in equation (2) has a negligible impact on  $V(\kappa_z)$  for  $\kappa_z < \kappa_W$ . The spectrum equation (3) corresponds to the well known saturated gravity waves model for  $\kappa_0 < \kappa_z < \kappa_W$  [e.g., *Smith et al.*, 1987]:

$$V_{\delta T/T} = A \frac{\omega_{BV}^4}{g^2} \kappa_z^{-3}, \kappa_z > 0, \quad (4)$$

where  $\omega_{BV}$  is the Brunt-Väisälä angular frequency and  $g$  is the acceleration of gravity. Hence the numerical parameter  $A$  in the saturated gravity wave model and the structure characteristic  $C_W$  are related by

$$C_W = \frac{3}{4\pi} A \frac{\omega_{BV}^4}{g^2}. \quad (5)$$

In the gravity wave literature, GW potential energy per unit mass  $E_p = \frac{1}{2} \left(\frac{g}{\omega_{BV}}\right)^2 \langle (\delta T/T)^2 \rangle$  is frequently used as a parameter quantifying gravity wave activity. For the model equation (2), computing variance of relative temperature fluctuations as  $\langle (\delta T/T)^2 \rangle = \iint \iint \Phi_W d\kappa_x d\kappa_y d\kappa_z = \int_{-\infty}^{\infty} V(\kappa_z) d\kappa_z$ , we get

$$E_p = \frac{2\pi}{3} \left(\frac{g}{\omega_{BV}}\right)^2 C_W \kappa_0^{-2}. \quad (6)$$

According to equations (3)–(6), parameter  $C_W$  specifies an intensity of “saturated” (short) waves  $\kappa_z > \kappa_0$ , whereas  $E_p$  depends also on the longest waves close to the outer scale.

[9] The second component of the spectrum equation (1) of air density irregularities,  $\Phi_K$ , corresponds to isotropic irregularities generated by turbulence, which appear as a

result of internal-wave breaking and/or different instabilities of atmospheric motions. For its parameterization, we use the Oboukhov-Corssin model of locally isotropic turbulence [*Monin and Yaglom*, 1975]:

$$\Phi_K(k) = 0.033 C_K k^{-11/3} \exp\left(-k/\kappa_K\right)^2, k^2 = \kappa_x^2 + \kappa_y^2 + \kappa_z^2, \quad (7)$$

where  $C_K$  is the structure characteristic of the random refractivity field and  $\kappa_K$  is the inner scale of isotropic irregularities,  $C_K = C_T^2 / \langle T \rangle^2$ , where  $C_T$  is the structure characteristic of the temperature field. The 1D spectrum corresponding to equation (7) follows the well-known  $-5/3$  power law for  $\kappa < \kappa_K$ . The analyses of scintillation data [*Gurvich and Kan*, 2003a, 2003b; *Gurvich and Chunchuzov*, 2005; *Sofieva et al.*, 2007a, 2007b] have shown the presence of both types of irregularity in the stratosphere.

[10] The modeled scintillation spectra based on equations (1), (2), and (7) can be computed using the theory of wave propagation in random media. The corresponding formulae for scintillation spectra and discussion of their behavior are presented by *Sofieva et al.* [2007a], along with the discussion on how many parameters can be retrieved from GOMOS scintillations. The anisotropy coefficient  $\eta$  cannot be retrieved from moderately oblique occultations (majority of GOMOS data) due to insensitivity of scintillation spectra to this parameter when  $\eta > 30$ . The algorithm for reconstruction of the four parameters of this spectral model - the structure characteristics  $C_K$  and  $C_W$  (for turbulence and waves), the characteristic wavenumbers  $\kappa_W$  and  $\kappa_0$  corresponding to the inner and outer scales of the GW component, respectively - is described in detail by *Sofieva et al.* [2007a]. It is based on fitting modeled scintillation spectra to measured spectra using the maximum likelihood method. The geometry of line of sight movement in each occultation is taken into account in fitting scintillation spectra [*Sofieva et al.*, 2007a], thus the retrieved vertical scales do not depend on occultation geometry.

### 3. Results and Discussion

[11] The nighttime occultations of the 30 brightest stars were selected for the analysis. In this paper, we show the distributions of GW parameters in two seasons of 2003, January–March and December and June–September. Locations of the occultations are shown in Figure (altogether 8215 occultations). The summer polar atmosphere is not covered, because only nighttime occultations were used. In this paper we restricted ourselves by considering zonal mean values only, in order to analyze the dependence on latitude and season. The in-depth analysis (including zonal inhomogeneity) of the whole data set will be presented in future publications. For data averaging, we calculated zonal means in latitudinal bins distributed in accordance with available data (Figure 1). The width of latitudinal bins is mainly  $\sim 10^\circ$ , but it ranges from  $5^\circ$  to  $30^\circ$ . Each latitudinal bin includes  $\sim 100$ – $200$  profiles.

[12] Figures 2a and 2b show the latitudinal distribution of the zonal mean GW structure characteristic  $C_W$  in the altitude range 30–47 km.  $C_W$  characterizes the strength of anisotropic irregularities, which are assumed to be generated by GW. The mean uncertainty of  $C_W$  in individual retrievals

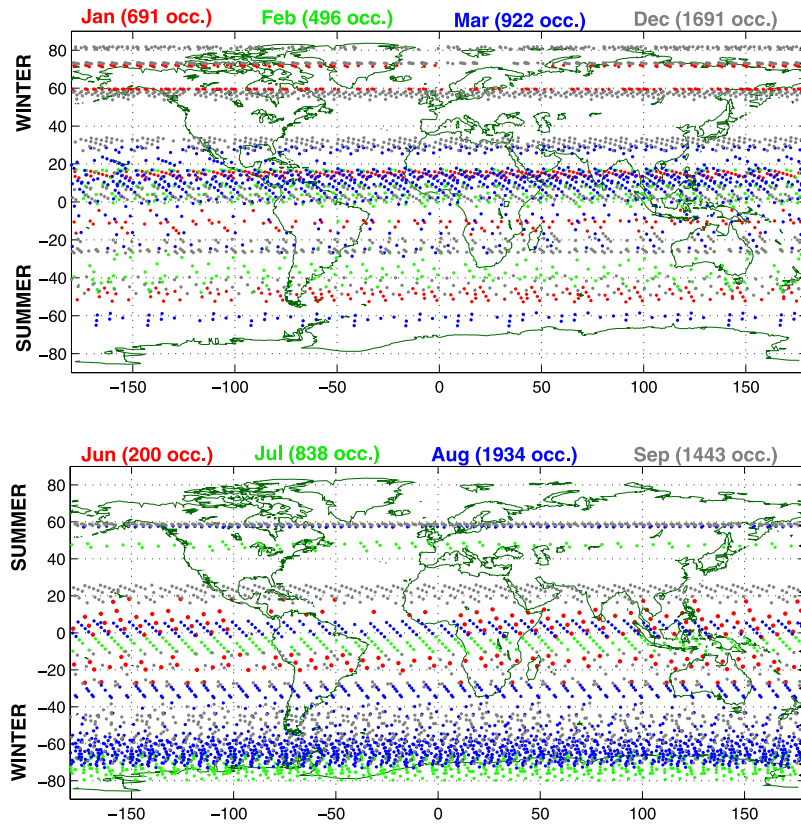


**Figure 1.** Location of selected occultations (altogether, 8215 occultations). The filled triangles on the right side indicate the centers of latitudinal bins used for data averaging.

estimated by the inverse problem solving procedure [Sofieva *et al.*, 2007a] is  $\sim 5\text{--}10\%$  in the majority of cases. At winter high latitudes above  $\sim 40$  km, if the anisotropic component of scintillation is masked by the isotropic one due to frequent presence of strong turbulence [Sofieva *et al.*, 2007b], the accuracy of  $C_W$  reconstruction worsens and can grow to 20–30% in individual occultations.

[13] Although a small increase of  $C_W$  with altitude can be observed, the main variations are in the latitudinal direction. Strong enhancements of  $C_W$  at mid and high latitudes in winter are observed, in both hemispheres. The enhancement is especially large in the Southern Hemisphere. Note that winter measurements at high latitudes in NH were carried out only in January or in December 2003 (Figure 1 (top)). In both months, major sudden stratospheric warmings (SSW) occur. Due to reversal of zonal winds accompanying SSW and thus unfavorable conditions for GW propagation in the stratosphere during these periods, the gravity wave activity is expected to be lower than for winters without major SSW (see also below).

[14] The annual cycle in gravity wave energy at altitudes 30–50 km at high and mid latitudes with a maximum in winter and a minimum in summer was observed previously in rocket sounding (with resolution  $\sim 1$  km) [Hamilton, 1991, Eckermann *et al.*, 1995], lidar data (resolution  $\sim 1$  km) [Wilson *et al.*, 1991; Whiteway and Carswell, 1995], and radiosonde data for altitudes 19–25 km [Tsuda *et al.*, 1991]. It has been discussed that the mean atmospheric conditions largely induce horizontal, vertical and temporal variations of the gravity wave field in the stratosphere and mesosphere.

[15] Equation (5) predicts that the structure characteristic  $C_W$  is proportional to  $\omega_{BV}^4$ . However, the range of latitudinal variations of  $C_W$  at a selected altitude ( $C_W^{\max}/C_W^{\min} \approx 6$  in January–March, December and  $C_W^{\max}/C_W^{\min} \approx 11$  in June–September) is significantly larger than the range of the corresponding variations of  $\omega_{BV}^4$  ( $\omega_{BV,\max}^4/\omega_{BV,\min}^4 \approx 1.3$  in January–March, December and  $\omega_{BV,\max}^4/\omega_{BV,\min}^4 \approx 1.6$  in June–September). In these estimates, zonal averaged data of  $C_W$  (Figures 2a and 2b) are used. Values of  $\omega_{BV}$  were estimated using temperature data from ECMWF analysis. The variations in the thermal structure, as measured by the static stability parameter  $\omega_{BV}$ , cannot quantitatively explain the observed latitudinal pattern of  $C_W$ .

[16] Figures 2c and 2d show zonal mean values of the reconstructed inner scale  $l_W = \frac{2\pi}{k_W}$  in the altitude range 30–45 km. This scale gives an estimate of minimal vertical wavelengths for GW. Temperature irregularities of smaller size are related to turbulence generated by GW breaking. The data averaging was performed in the same way as for  $C_W$ . The mean estimated uncertainty of  $l_W$  in individual retrievals is  $\sim 5\text{--}15\%$  in the majority of the cases considered. The values of  $l_W$  grow with altitude, from  $\sim 10$  m at 30 km up to 40–70 m above 40 km. It can be noticed that the values of  $l_W$  are slightly smaller at high latitudes in winter, compared to other locations and seasons. There are enhancements of  $l_W$  in equatorial regions at altitudes  $>40$  km. The position of these maxima follows sub-solar latitude.

[17] Figures 2e and 2f show zonal mean values of the reconstructed outer scale  $L_0$ . The values of  $L_0$  are shown for the altitude range 30–42 km. At higher altitudes, the outer

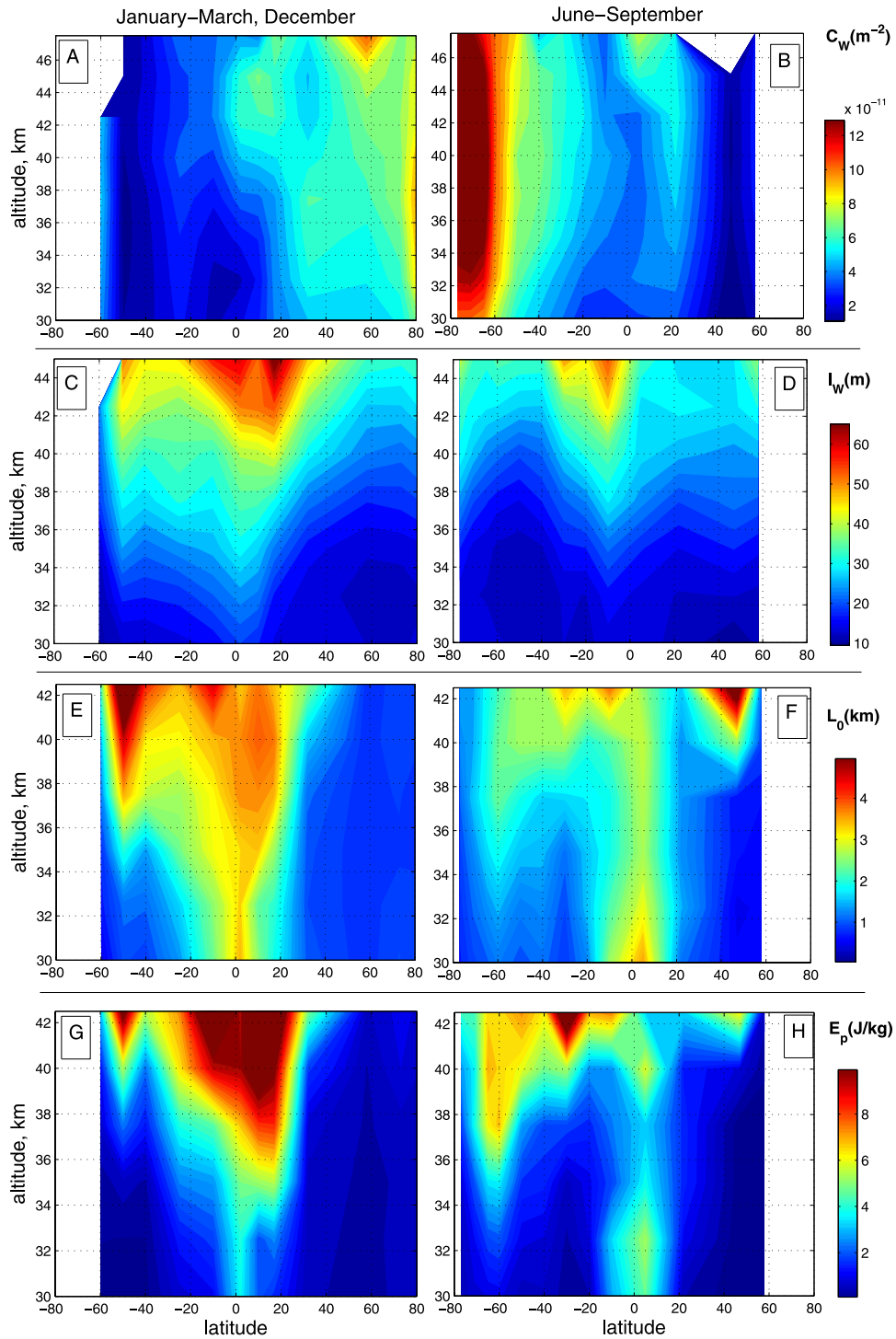


**Figure 2.** Zonal mean values of: (a and b)  $C_w$ , (c and d)  $I_w$ , (e and f)  $L_0$ , and (g and h)  $E_p$  for (left) Jan–Mar, Dec and (right) Jun–Sep.

scale is often not observed in the scintillation spectra, thus the retrieval accuracy is poor. At altitudes 30–42 km, the mean accuracy in individual  $L_0$  retrievals is estimated to be 15–35% at altitudes 30–37 km and 35–60% at altitudes above 37 km. We recall that the outer scale was introduced as characterizing the low wavenumber limit of the  $\kappa^{-3}$  spectrum equation (3). The mean value of retrieved  $L_0$  grows with altitude, from 0.5–1 km at 30 km up to 2–4 km

at 40–42 km, thus being in qualitative agreement with the theoretical prediction that the dominant vertical scales should increase with altitude [Fritts and Alexander, 2003]. The retrieved values of outer scale are in the range of the estimates for possible values of  $L_0$  [Gurvich and Chunchuzov, 2005]. They are also in the range of dominant vertical wavelengths, as obtained from lidar data at 30–40 km and from radiosonde data at lower stratospheric altitudes [Chane-Ming *et al.*,

2000]. The range of dominant wavelengths obtained from different measurements [Chane-Ming *et al.*, 2000, Table 2] is quite large, from  $\sim 1$  km up to 10–15 km. We would like to note that very large temperature irregularities (with vertical scales of the order of magnitude of atmospheric scale) produce disturbances in observed stellar flux that are impossible to distinguish from the mean refractive dilution. For this reason, the method used does not yield reliable estimates of very large  $L_0$  comparable with the atmospheric scale of 6–7 km, thus the estimate of mean  $L_0$  can be biased toward small values. The global distributions of  $L_0$  exhibit marked enhancements in the equatorial regions, in both seasons.

[18] The value of outer scale has a determining influence on potential energy, as it follows from equation (6). However, experimental estimation of outer scale is difficult when using temperature profiles or temperature spectra. Thus a fixed prior estimate of outer scale is used in experimental determination of  $E_p$  from temperature profile fluctuations [e.g., Tsuda *et al.*, 2000; Wilson *et al.*, 1991; de la Torre *et al.*, 2006]. The problem of outer scale  $L_0$  estimations is simplified when using scintillations, because the outer scale can be retrieved directly from scintillation spectra.

[19] Figures 2g and 2h show zonal mean values of GW potential energy per unit mass. All values of  $E_p$  were calculated using equation (6), where  $\kappa_0$  is estimated from scintillation spectra. This makes estimations of  $E_p$  more representative, but also more dependent on the spectral model selected.

[20] The distributions of  $E_p$  shown in Figures 2g and 2h are in very good agreement with previous estimates of this parameter from radiosonde, lidar and GPS radio-occultation measurements, both qualitatively and quantitatively [Allen and Vincent, 1995; Tsuda *et al.*, 1991, 2000; de la Torre *et al.*, 2006]. In particular, enhancements in equatorial regions are clearly observed, analogous to those found in global analyses of radio-occultation data [de la Torre *et al.*, 2006; Tsuda *et al.*, 2000]. As seen in Figure 2, these equatorial enhancements of  $E_p$  are caused by large values of outer scale  $L_0$  at these locations (Figures 2e and 2f). Enhanced  $E_p$  in the SH winter high latitude stratosphere is observed, also in agreement with  $E_p$  estimated from radio-occultation data. Contrary to expectations, no enhancement of  $E_p$  at high-latitudes in winter is observed in Northern Hemisphere. It is probably caused by the fact that occultations at NH winter high latitudes were carried out in January 2003 and in December 2003, when the sudden stratospheric warmings lasted a significant part of the observational period. It is interesting to note that reduced GW activity during SSW was also observed earlier using lidar observations [Whiteway and Carswell, 1994]. The comparison of GW parameters at  $\sim 73$  N in Dec 2003 (SSW) and in Dec 2004 (no SSW) have confirmed (not shown in this paper) that the values of  $C_W$  are significantly larger in Dec 2004, for “normal” winter conditions. Multi-year comparisons – to be published in the future – will justify our assumption on the absence of  $E_p$  enhancement in the NH high-latitude winter stratosphere in 2003 caused by sudden stratospheric warmings during the observation period.

[21] In our method, the GW spectra parameters are reconstructed simultaneously with the structure characteristic of isotropic turbulence [Sofieva *et al.*, 2007a]. This allows

characterization of GW breaking in the atmosphere. The distributions of  $C_T^2$  obtained with the aid of reconstruction of parameters are practically identical to those obtained previously using the simplified spectral analysis [Gurvich *et al.*, 2007]. This confirms consistency of the simplified methods. Large values of  $C_T^2$  are observed at high latitudes in winter, especially in the Southern Hemisphere where they may reach  $0.006 \text{ K}^2 \text{ m}^{-2/3}$ , i.e., values that are comparable with those observed in the turbulent boundary layer. We think that the appearance of strong turbulence at altitudes above 40–45 km in the winter polar atmosphere is related to breaking of gravity waves in the polar night jet. This hypothesis discussed previously by Sofieva *et al.* [2007b] and Gurvich *et al.* [2007] is confirmed now also by quantitative estimates. However, the important problem of gravity wave breaking requires special attention. It will be considered in details in future publications.

#### 4. Summary

[22] In this paper, we have presented global distributions of the GW and turbulence spectra parameters in two seasons of 2003 retrieved from stellar scintillation measurements by GOMOS. We assumed a two-component spectral model of air density irregularities: the first component corresponds to an ensemble of gravity waves, while the second one describes locally isotropic turbulence resulting from GW breaking and other instabilities. The retrieval is based on reconstruction of GW and turbulence spectra parameters by fitting modeled scintillation spectra to measured spectra.

[23] We have shown global distributions and seasonal variations of the structure characteristic, inner and outer scales of the GW component, for altitudes 30–50 km.

[24] In addition, we show global distributions of GW potential energy per unit mass. At altitudes and locations overlapping with other measurements, the GW and turbulence parameters retrieved from scintillations are in good agreement with those obtained from other measurements. Our main findings and observations are:

[25] 1. A strong enhancement of  $C_W$  at high latitudes in winter is observed, which is especially large in the Southern Hemisphere.

[26] 2. Low values of  $C_W$  are associated with sudden stratospheric warmings.

[27] 3. Both inner and outer scales grow with altitude. The distributions have enhancements in equatorial regions.

[28] 4. Measured values of outer scale lead to estimates of GW potential energy per unit mass  $E_p$ . Enhanced values of  $E_p$  are observed in equatorial regions and at SH high latitudes in winter above 35 km.

[29] Since other measurements at such small scales are very scarce at these altitudes, the global distributions obtained provide unique and complementary information about small-scale air density irregularities in the stratosphere. Future multi-year analysis will refine the observations and will provide information about spatial and interannual variability of GW and turbulence spectra parameters in the stratosphere.

[30] **Acknowledgments.** The authors thank ESA, ACRI-ST and the GOMOS team for the GOMOS data. The work of VS was supported by the Academy of Finland. The work of AG was supported by RFBR grant 06-05-64357.

## References

- Allen, S. J., and R. A. Vincent (1995), Gravity wave activity in the lower atmosphere: Seasonal and latitudinal variations, *J. Geophys. Res.*, *100*, 1327–1350.
- Chane-Ming, F., F. Molinaro, J. Leveau, P. Keckhut, and A. Hauchecorne (2000), Analysis of gravity waves in the tropical middle atmosphere over La Reunion Island (21°S, 55°E) with lidar using wavelet techniques, *Ann. Geophys.*, *18*, 485–498.
- de la Torre, A., T. Schmidt, and J. Wickert (2006), A global analysis of wave potential energy in the lower stratosphere derived from 5 years of GPS radio occultation data with CHAMP, *Geophys. Res. Lett.*, *33*, L24809, doi:10.1029/2006GL027696.
- Eckermann, S. D., I. Hirota, and W. K. Hocking (1995), Gravity wave and equatorial wave morphology of the stratosphere derived from long-term rocket soundings, *Q.J.R. Meteorol. Soc.*, *121*, 149–186.
- Fritts, D. C., and M. J. Alexander (2003), Gravity wave dynamics and effects in the middle atmosphere, *Rev. Geophys.*, *41*(1), 1003, doi:10.1029/2001RG000106.
- Gurvich, A., and I. Chunchuzov (2005), Estimates of characteristic scales in the spectrum of internal waves in the stratosphere obtained from space observations of stellar scintillations, *J. Geophys. Res.*, *110*, D03114, doi:10.1029/2004JD005199.
- Gurvich, A. S., and V. Kan (2003a), Structure of air density irregularities in the stratosphere from spacecraft observations of stellar scintillation: 1. Three-dimensional spectrum model and recovery of its parameters, *Izv. Russ. Acad. Sci. Atmos. Oceanic Phys.*, *39*, 300–310.
- Gurvich, A. S., and V. Kan (2003b), Structure of air density irregularities in the stratosphere from spacecraft observations of stellar scintillation: 2. Characteristic scales, structure characteristics, and kinetic energy dissipation, *Izv. Russ. Acad. Sci. Atmos. Oceanic Phys.*, *39*, 311–321.
- Gurvich, A. S., V. F. Sofieva, and F. Dalaudier (2007), Global distribution of  $C_2^*$  at altitudes 30–50 km from space-borne observations of stellar scintillation, *Geophys. Res. Lett.*, *34*, L24813, doi:10.1029/2007GL031134.
- Hamilton, K. (1991), Climatological statistics of stratospheric inertia-gravity waves deduced from historical rocketsonde wind and temperature data, *J. Geophys. Res.*, *96*, 20,831–20,839.
- Monin, A. S., and A. M. Yaglom (1975), *Statistical Fluid Mechanics*, vol. 2, MIT Press, Cambridge, Mass.
- Smith, S. A., D. C. Fritts, and T. E. VanZandt (1987), Evidence of a saturation spectrum of atmospheric gravity waves, *J. Atmos. Sci.*, *44*, 1404–1410.
- Sofieva, V. F., A. S. Gurvich, F. Dalaudier, and V. Kan (2007a), Reconstruction of internal gravity wave and turbulence parameters in the stratosphere using GOMOS scintillation measurements, *J. Geophys. Res.*, *112*, D12113, doi:10.1029/2006JD007483.
- Sofieva, V. F., et al. (2007b), Global analysis of scintillation variance: Indication of gravity wave breaking in the polar winter upper stratosphere, *Geophys. Res. Lett.*, *34*, L03812, doi:10.1029/2006GL028132.
- Tatarskii, V. I. (1971), *The Effects of the Turbulent Atmosphere on Wave Propagation*, 417 pp., U.S. Dep. of Commer., Washington, D. C.
- Tsuda, T., T. E. VanZandt, M. Mizumoto, S. Kato, and S. Fukao (1991), Spectral analysis of temperature and Brunt-Väisälä frequency fluctuations observed by radiosondes, *J. Geophys. Res.*, *96*, 17,265–17,278.
- Tsuda, T., M. Nishida, C. Rocken, and R. H. Ware (2000), A global morphology of gravity wave activity in the stratosphere revealed by the GPS occultation data (GPS/MET), *J. Geophys. Res.*, *105*, 7257–7273.
- Whiteway, J. A., and A. I. Carswell (1994), Rayleigh lidar observations of thermal structure and gravity wave activity in the high Arctic during a stratospheric warming, *J. Atmos. Sci.*, *51*, 3122–3136.
- Whiteway, J. A., and A. I. Carswell (1995), Lidar observations of gravity wave activity in the upper stratosphere over Toronto, *J. Geophys. Res.*, *100*, 14,113–14,124.
- Wilson, R., M. L. Chanin, and A. Hauchecorne (1991), Gravity waves in the middle atmosphere observed by Rayleigh lidar: 2. Climatology, *J. Geophys. Res.*, *96*, 5153–5167.

F. Dalaudier, LATMOS, BP 3, F-91371 Verrières-le-Buisson CEDEX, France.

A. S. Gurvich, A. M. Oboukhov Institute of Atmospheric Physics, Pyzhevsky 3, Moscow 119017, Russia.

V. F. Sofieva, Finnish Meteorological Institute, P. O. Box 503, FIN-00101 Helsinki, Finland. (viktorija.sofieva@fmi.fi)